IET Power Electronics

Research Article

IET Journals
The Institution of Engineering and Technology

Soft switched full-bridge light emitting diode driver configuration for street lighting application

ISSN 1755-4535
Received on 8th January 2017
Revised 12th August 2017
Accepted on 31st August 2017
E-First on 24th November 2017
doi: 10.1049/iet-pel.2017.0021
www.ietdl.org

Ch Kasi Ramakrishnareddy[1], Porpandiselvi Shunmugam[1] ✉, Neti Vishwanathan[1]

[1]*Department of Electrical Engineering, National Institute of Technology, Warangal, India*

✉ *E-mail: porpandiselvi@gmail.com*

Abstract: This study presents a light emitting diode driver circuit topology based on a full-bridge configuration with dimming control. It is more suitable for high power lighting loads. The proposed configuration has advantages of zero-voltage switching, reduced component count and high efficiency. It can power multiple lighting loads. Operation of the proposed circuit configuration is explained in detail and it is validated through simulated and experimental results on the 145 W experimental prototype with dimming control.

1 Introduction

Lighting loads consume around 19% of the electrical energy generated [1]. In order to save electrical energy, the lighting system should be designed with high efficiency. Usage of light emitting diodes (LEDs) for lighting application is one of the ways of making the system efficient. Recently, LEDs have become a popular source of illumination due to their long lifetime, higher luminous efficiency, ease of controllability, compactness and good colour rendering property [2–4]. LEDs are used in applications like traffic lighting, street lighting, domestic lighting, automotive lighting, decorative lighting and so on [5, 6].

The illumination level of LEDs directly depends on its forward current [7]. Hence, this current needs to be controlled accurately. LEDs can be powered with either linear or switching power regulators. Switching regulators are more preferred due to high efficiency [8–10]. A good number of converter configurations have been proposed for powering LEDs [11–15]. Desirable features of the LED power drivers are high conversion efficiency, ease of control of dimming and so on. Converters without electrolytic capacitors are preferable. In [16], a two-input buck converter-based LED driver has been proposed, with reduced voltage stress of switching devices and improved efficiency. Garcia *et al*. [17] propose an interleaved scheme for LED driver where ripple current reduction is possible with relatively lower values of reactive components. In [18, 19], a virtual voltage source and a series connection of current regulator are proposed which helps in reducing the power loss in LED drivers. Converters with soft switching techniques are also used in LED drivers to increase the power conversion efficiency. A switched capacitor converter with zero-current switching (ZCS) is proposed in [20] for LED driver applications. Wang *et al*. [21] propose a dc–dc resonant converter for powering LEDs. In [22, 23], a class-D resonant converter with zero-voltage switching (ZVS) is proposed for outdoor applications. Driver circuits are proposed for multiple LED string applications based on full-bridge dc–dc resonant topology in [24, 25]. A low power and cost effective resonant assisted buck converter is designed for LED applications in [26].

Dimming feature is incorporated in lighting applications which helps in saving of electrical energy. Commonly used dimming techniques for LEDs include amplitude modulation (AM) [27], pulse-width modulation (PWM) [28, 29], hybrid AM/PWM control [30], double PWM [18, 19], multiphase PWM [31], integral cycle control [32], and bi-level current control [33]. These techniques have their own advantages and limitations.

Despite the availability of several converter configurations and control techniques, there is enough scope for further research in making a compact LED power driver with reduced components count, high efficiency and dimming control to suit various application needs. This paper proposes an LED driver using bridge configuration with ZVS [34]. It can be used for high power lighting applications like street lighting application with dimming control. It uses on–off technique for dimming control. It offers high efficiency due to reduced switching and conduction losses. It does not require any additional rectifier stage. The principle of operation of the proposed circuit is explained in Section 2. Analysis of the operation of proposed LED driver is discussed in Section 3. In Section 4, the design procedure is described. Dimming and regulation features are presented in Section 5. Simulation and experimental results are presented in Section 6. Section 7 states the conclusions of the proposed LED driver.

2 Principle of operation of proposed LED driver

Fig. 1*a* shows the circuit diagram of the proposed LED driver. This circuit uses a full-bridge configuration consisting of four power metal–oxide–semiconductor field-effect transistors (MOSFETs) S_1, S_2, S_3, and S_4. D_1–D_4 are the intrinsic body diodes of power MOSFETs and C_1–C_4 indicate either the output capacitances of power MOSFETs or external capacitors. The series connection of LEDs and an inductor is in parallel with each switch. Each LED lamp represents a dc load and can be considered as one street light lamp. In proposed circuit, four LED lamps are present. The number of LED lamps can be increased by the addition of more legs. The inductors L_1, L_2, L_3, and L_4 are designed to provide continuous current through lamp-1, lamp-2, lamp-3, and lamp-4, respectively. The inductor L_r is used to obtain ZVS in all the four switches. The switches S_1 and S_2 are alternately turned on and off at a switching frequency $f_s = 1/T$ with 50% duty ratio. Similarly, S_3 and S_4 are alternately turned on and off at the same switching frequency with 50% duty ratio. To avoid short circuit across the dc power supply, a dead time is provided between switching pulses of S_1 and S_2. As the dead times are very small, the lamp currents and inductor current i_{Lr} are assumed to be constant during dead time. The switch S_d incorporates dimming feature by using a low-frequency gate signal. The input voltage V_{in} to the bridge is obtained from three dc voltages V_{DC1}, V_{DC2}, and V_C. V_{DC2} is the input voltage to the buck–boost converter and V_C is its output voltage. V_{DC1} must be far greater than the summation of remaining dc voltages, i.e. ($V_{DC2} + V_C$) to reduce the power handled by buck–boost converter. The dc voltage sources V_{DC1} and V_{DC2} can be obtained from rechargeable batteries. For any variations in supply voltage, input

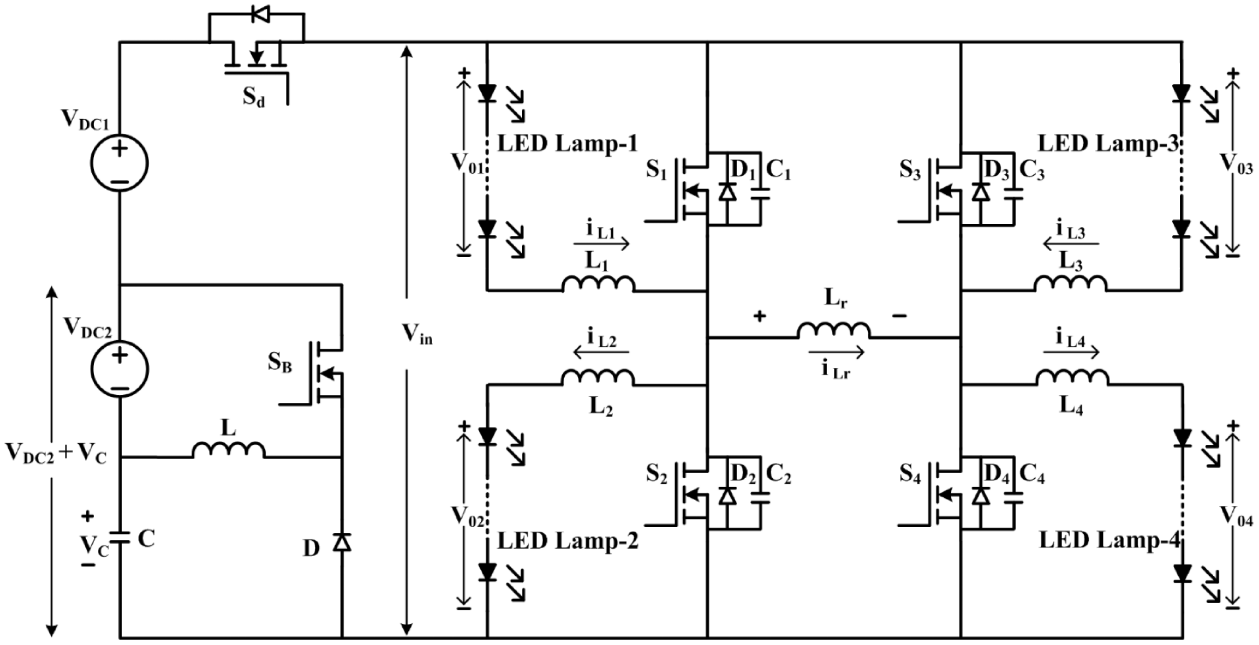

a

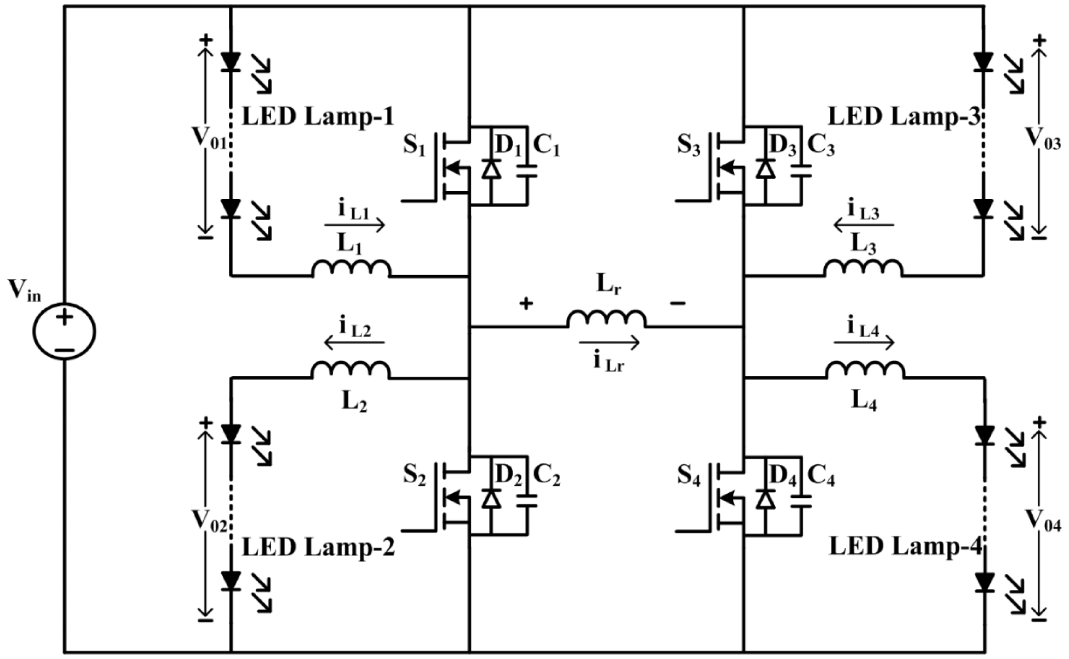

b

Fig. 1 *Continued*

voltage v_{in} is controlled to be constant by the buck–boost converter. To understand the working principle of the proposed LED driver, the simplified circuit diagram shown in Fig. 1*b*, where the input voltage V_{in} is represented by a voltage source. Fig. 1*c* shows the operating waveforms of the proposed LED driver. Fig. 1*d* shows an extension of proposed configuration to multiple LED lamps. The equivalent circuits in different working modes in a switching cycle are shown in Figs. 2 and 3. The working modes are explained in this section.

2.1 Mode I: (t_0–t_1)

At time instant t_0, switches S_1 and S_4 are turned on at zero voltage. LED lamp-2 and lamp-3 are powered by input voltage V_{in}. LED lamp-1 and lamp-4 are supplied by energy stored in inductors L_1 and L_4, respectively. Due to the nature of inductor L_r, the current i_{Lr} linearly increases through the switches S_1 and S_4. Currents through lamp-2 and lamp-3 increase and currents through lamp-1 and lamp-4 decrease linearly. As all LED lamps are identical, average lmp current values are equal. The difference of i_{L2} and i_{L1} which is of a small value flows through S_1. Similarly, a difference of i_{L3} and i_{L4} flows through S_4. Hence devices are conducting only a small value of current. This reduces device current stress and conduction losses. This mode ends when inductor current i_{Lr} becomes zero.

2.2 Mode II: (t_1–t_2)

The explanation in Mode I is valid for this mode also except that the current i_{Lr} increases from zero to positive maximum through the switches S_1 and S_4. This mode ends at t_2.

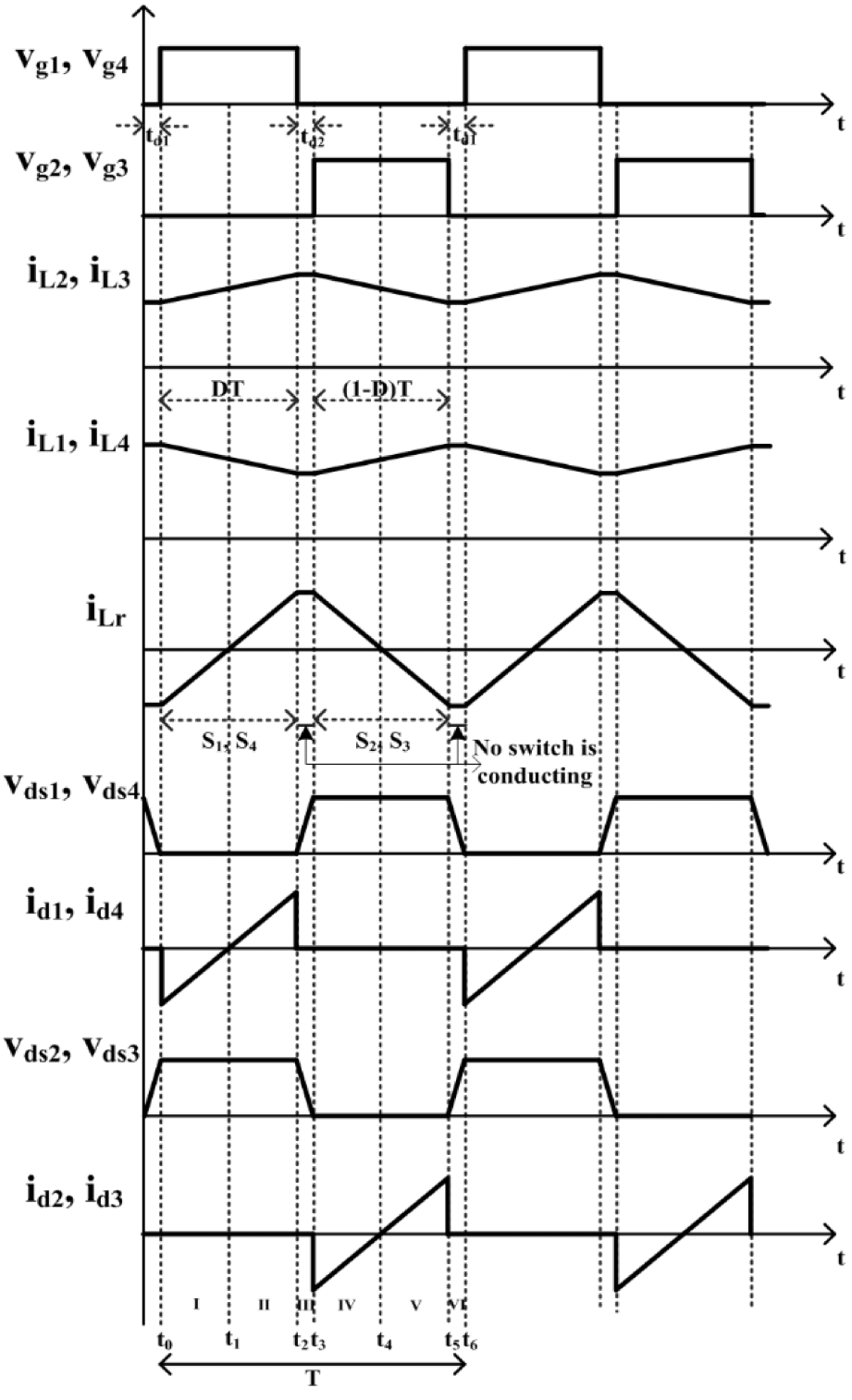

c

Fig. 1 *Continued*

2.3 Mode III: (t_2–t_3)

This mode begins after removing gate signals for switches S_1 and S_4, which are carrying positive currents. Switches S_1 and S_4 are turned off at zero voltage. During t_2 to t_3, none of the switches is conducting. Current $(i_{Lr}+i_{L2}-i_{L1})/2$ charges the capacitor C_1 and discharges the capacitor C_2. Similarly, $(i_{Lr}+i_{L3}-i_{L4})/2$ charges the capacitor C_4 and discharges the capacitor C_3. After this, D_2 and D_3 start conducting. Now the switches S_2 and S_3 may be turned on with ZVS. This mode ends when capacitors C_2 and C_3 are discharged from V_{in} to zero or C_1 and C_4 are charged from zero to V_{in}.

2.4 Mode IV: (t_3–t_4)

At time instant t_4, switches S_2 and S_3 are turned on at zero voltage. LED lamp-1 and lamp-4 are powered by input voltage V_{in}. LED lamp-2 and lamp-3 are supplied by energy stored in inductors L_2 and L_3, respectively. Due to the nature of inductor L_{r}, the current i_{Lr} decreases through the switches S_2 and S_3. Currents through lamp-1 and lamp-4 increase and currents through lamp-2 and lamp-3 decrease linearly. Difference between i_{L1} and i_{L2} flows through the switch S_2 and difference between i_{L4} and i_{L3} flows through the switch S_3. As the device current is less, device current

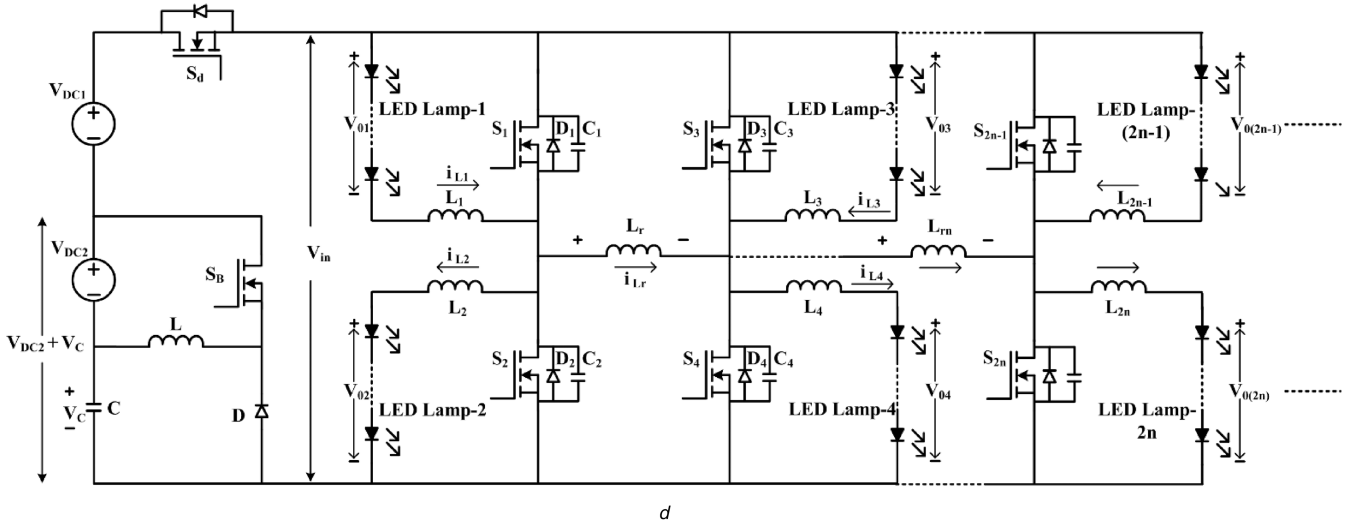

d

Fig. 1 *Circuit diagram and waveforms*
(a) Proposed LED driver, ***(b)*** Simplified circuit diagram, ***(c)*** Operating waveforms, ***(d)*** Extension to multiple LED lamps

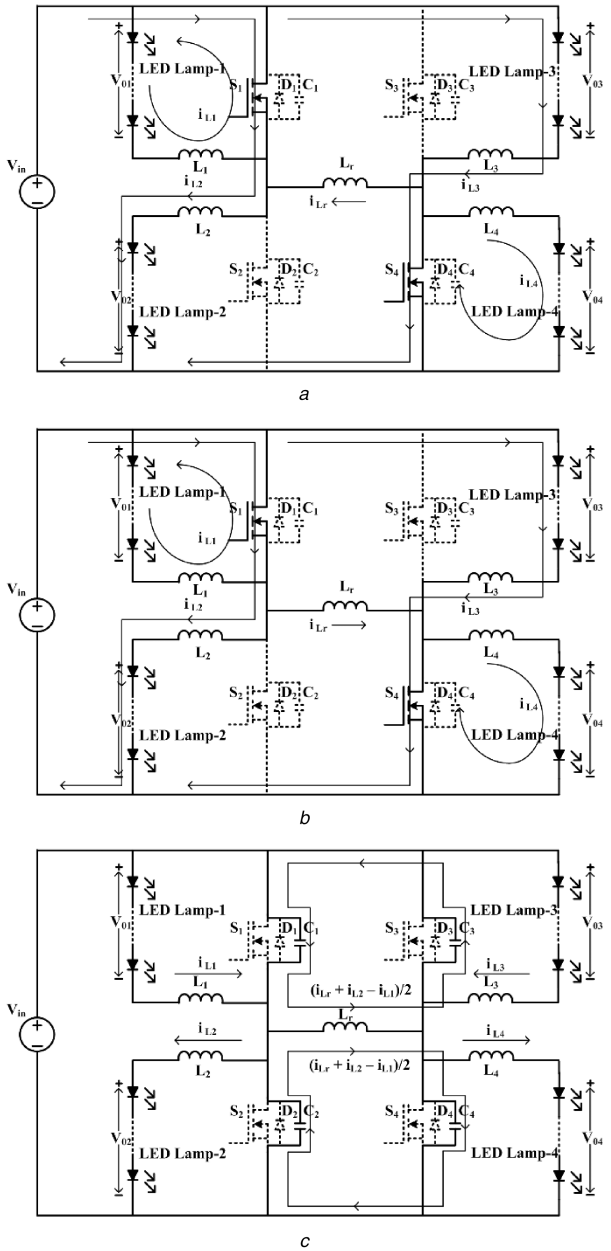

a

b

c

Fig. 2 *Equivalent circuits of proposed LED driver when S_1 and S_4 are ON*
(a) Mode-I, ***(b)*** Mode-II, ***(c)*** Mode-III

stress and conduction losses are reduced. This mode ends when current i_{Lr} becomes zero.

2.5 Mode V: (t_4–t_5)

The explanation in Mode IV is valid for this mode also except that the current i_{Lr} decreases from zero to negative maximum through the switches S_2 and S_3. This mode ends at t_5.

2.6 Mode VI: (t_5–t_6)

This mode begins after removing gate signals for switches S_2 and S_3, which are carrying positive currents. The process of turning off of switches S_2, S_3 and turning on of switches S_1, S_4 with zero voltage is similar to that in Mode III. This mode ends when capacitors C_1 and C_4 are discharged from V_{in} to zero or C_2 and C_3 are charged from zero to V_{in}.

3 Analysis of the proposed LED driver

The analysis of the proposed LED driver is carried out by considering the following assumptions:

i. The proposed converter is operating in steady state.
ii. The circuit components are ideal.
iii. All four LED lamps are identical.
iv. The voltage across each LED lamp is constant.

The switches are operated with a fixed duty cycle at a fixed frequency. Each switch is on for 50% duty cycle and off for a remaining period. To calculate the voltage across each LED lamp, it is essential to examine the inductor currents and voltages. As the LED lamps and their operating currents are identical, the analysis is shown for a single LED lamp, i.e. LED lamp-2. When the switches S_1 and S_4 are ON and S_2 and S_3 are OFF, the LED lamp-2 is supplied by input dc voltage V_{in} through the inductor L_2. The corresponding equivalent circuits are shown in Figs. 2*a* and *b*.

3.1 Mode-I and Mode-II (t_0–t_2)

The voltage across inductor L_2 is expressed as

$$v_{L2} = V_{\text{in}} - V_{02} = L_2 \frac{\mathrm{d}i_{L2}}{\mathrm{d}t} \quad t_0 \le t < t_2 \tag{1}$$

The current through the inductor L_2 is

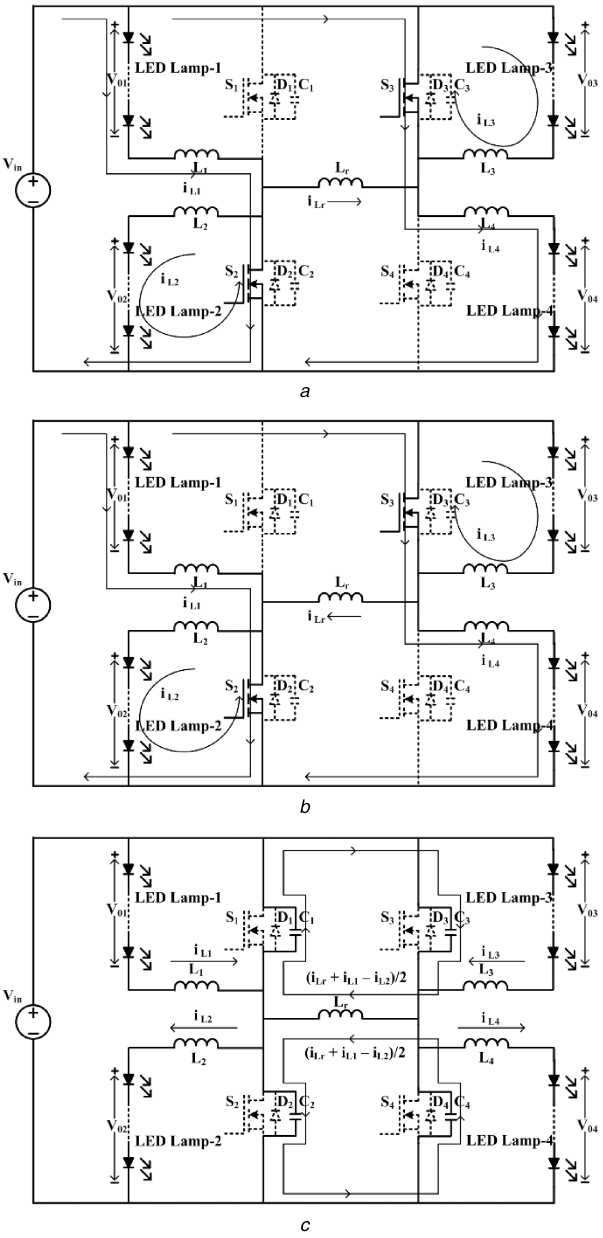

Fig. 3 *Equivalent circuits of proposed LED driver when S_2 and S_3 are ON*
(a) Mode-IV,
(b) Mode-V,
(c) Mode-VI

$$i_{L2}(t) = \frac{1}{L_2}\int_{t_0}^{t} v_{L2}(t)\mathrm{d}t + i_{L2}(t_0) = \frac{V_{\text{in}} - V_{02}}{L_2}(t - t_0) + i_{L2}(t_0) \quad t_0 \le t < t_2 \tag{2}$$

where $i_{L2}(t_0)$ is the initial current in the inductor L_2 at time $t = t_0$. At $t = t_2$, $i_{L2}(t)$ reaches maximum value, which is

$$i_{L2}(t_2) = \frac{V_{\text{in}} - V_{02}}{L_2}(t_2 - t_0) + i_{L2}(t_0) \tag{3}$$

The duration $(t_2 - t_0)$ is the ON period of switches S_1 and S_4. Hence (3) can be written as

$$i_{L2}(t_2) = \frac{V_{\text{in}} - V_{02}}{L_2}DT + i_{L2}(t_0) \tag{4}$$

where D is duty ratio of switches S_1 and S_4 and T is the switching period.

From (4), the ripple current in inductor L_2 is expressed as

$$\Delta i_{L2} = i_{L2}(t_2) - i_{L2}(t_0) = \frac{V_{\text{in}} - V_{02}}{L_2}DT \tag{5}$$

During this interval, the voltage across L_{r} is V_{in}. The current through it increases linearly and is expressed as

$$i_{Lr}(t) = \frac{V_{\text{in}}}{L_r}(t - t_0) + i_{Lr}(t_0) \quad t_0 \le t < t_2 \tag{6}$$

3.2 Mode-IV and Mode-V (t_3–t_5)

When the switches S_1 and S_4 are switched-off and S_2 and S_3 are switched-on, the LED lamp-2 is supplied by the stored energy in the inductor L_2. The corresponding equivalent circuits are shown in Figs. 3*a* and *b*.

The voltage across inductor L_2 is

$$v_{L2} = -V_{02} = L_2\frac{\mathrm{d}i_{L2}}{\mathrm{d}t} \quad t_3 \le t < t_5 \tag{7}$$

The current through the inductor L_2 is expressed as

$$\begin{aligned} i_{L2}(t) &= \frac{1}{L_2}\int_{t_3}^{t} v_{L2}(t)\mathrm{d}t + i_{L2}(t_3) \\ &= \frac{-V_{02}}{L_2}(t - t_3) + i_{L2}(t_3) \quad t_3 \le t < t_5 \end{aligned} \tag{8}$$

where $i_{L2}(t_3)$ is the initial current in the inductor L_2 at time $t = t_3$. At $t = t_5$, $i_{L2}(t)$ reaches minimum value and is given by

$$i_{L2}(t_5) = \frac{-V_{02}}{L_2}(t_5 - t_3) + i_{L2}(t_3) \tag{9}$$

Assuming that dead time t_{d1} and t_{d2} are negligible, the duration $(t_5 - t_3)$ is the OFF period of switches S_1 and S_4. Equation (9) can be written as

$$i_{L2}(t_5) = \frac{-V_{02}}{L_2}(1 - D)T + i_{L2}(t_3) \tag{10}$$

From (10), the ripple current in inductor L_2 is expressed as

$$\Delta i_{L2} = i_{L2}(t_5) - i_{L2}(t_3) = \frac{-V_{02}}{L_2}(1 - D)T \tag{11}$$

During this interval, the voltage across L_{r} is $-V_{\mathrm{in}}$. The current through it decreases linearly and is given by

$$i_{Lr}(t) = -\frac{V_{\mathrm{in}}}{L_r}(t - t_3) + i_{Lr}(t_3) \quad t_3 \le t < t_5 \tag{12}$$

Under steady-state operation, the net change in current through inductor L_2 is zero over the time period T. Hence from (5) and (11)

$$[i_{L2}(t_2) - i_{L2}(t_0)] + [i_{L2}(t_5) - i_{L2}(t_3)] = 0 \tag{13}$$

$$\Rightarrow \frac{V_{\mathrm{in}} - V_{02}}{L_2}DT - \frac{V_{02}}{L_2}(1 - D)T = 0 \tag{14}$$

$$\Rightarrow V_{02} = DV_{\mathrm{in}} \tag{15}$$

Hence, the voltage across the LED lamp V_{02} is D times the input voltage V_{in}. The analysis for other LED lamps is similar to the aforementioned analysis. Equations (5), (11), and (15) are applicable to other LED lamps also. Hence, the ripple current through each LED lamp and voltage across each LED lamp are given by

$$\Delta i_{Lk} = \frac{V_{\mathrm{in}} - V_{0k}}{L_k}DT = \frac{-V_{0k}}{L_k}(1 - D)T \tag{16}$$

where $k = 1, 2, 3, 4$

$$V_{0k} = DV_{\mathrm{in}} \tag{17}$$

where $k = 1, 2, 3, 4$

The value of inductor for specified current ripple can be determined from (16) under continuous current.

4 Design considerations

An LED can be represented by a series connection of an equivalent resistance r_{d}, an equivalent voltage V_{th} and an ideal diode [35]. In the proposed work four LED lamps are used. Each LED lamp comprises of two strings of LEDs which are connected in parallel. In each string, ten LEDs are connected in series. Each LED is operated at 3.3 V, 550 mA, and 1.815 W. Each LED lamp is operated at 33 V, 1.1 A, and 36.3 W.

From (17), input voltage V_{in} is given by

$$V_{\mathrm{in}} = \frac{V_{0k}}{D} \tag{18}$$

With a duty ratio of 0.5, and V_{0k} of 33 V, the input voltage is calculated as $V_{\mathrm{in}} = 66$ V.

Rearranging (16)

$$L_k = \frac{V_{\mathrm{in}} - V_{0k}}{\Delta i_{Lk}}DT, \quad k = 1, 2, 3, 4 \tag{19}$$

With $V_{\mathrm{in}} = 66$ V, $V_{0k} = 33$ V, $D = 0.5$, $T = 5$ µs, peak-to-peak LED current Δi_{Lk} of 13%, the value of inductor L_k is calculated as $L_k \cong 577\ \mu$H.

To ensure ZVS during dead time, the appropriate current magnitude is required to charge and discharge the output capacitors of the switches [36]. The inductor L_{r} is used to provide the required constant current during dead time. The peak current through L_{r} is assumed to be constant during dead time. At $t = t_2$, $i_{Lr}(t)$ reaches a maximum value. Hence from (6)

$$\begin{aligned} i_{Lr-pk} &= \frac{V_{\mathrm{in}}}{L_r}(t_2 - t_0) + i_{Lr}(t_0) \\ &= \frac{V_{\mathrm{in}}}{L_r}(t_2 - t_0) - \frac{V_{\mathrm{in}}}{L_r}(t_1 - t_0) \end{aligned} \tag{20}$$

As $t_2 - t_0 = DT$ and $t_1 - t_0 = DT/2$, (20) can be written as

$$i_{Lr-pk} = \frac{V_{\mathrm{in}}}{L_{\mathrm{r}}}\left(DT - \frac{DT}{2}\right) = \frac{V_{\mathrm{in}}DT}{2L_{\mathrm{r}}} \tag{21}$$

With a duty ratio of 0.5, the peak current through the L_{r} is given by

$$i_{Lr-pk} = \frac{V_{\mathrm{in}}T}{4L_{\mathrm{r}}} \tag{22}$$

The value of i_{Lr-pk} is inversely proportional to inductor L_{r} for a fixed value of V_{in} and T. For $L_{\mathrm{r}} = 120$ µH, $V_{\mathrm{in}} = 66$ V, $T = 5$ µs, i_{Lr-pk} is calculated as $i_{Lr-pk} = 0.6875$ A.

For the calculation of the switch output capacitor value, the currents through L_k and current through L_{r} during dead time are assumed to be constant. Assuming that dead time $t_{\mathrm{d1}} = t_{\mathrm{d2}} = t_{\mathrm{d}}$, current flowing through output capacitors during t_{d1} or t_{d2} is given by

$$i_{Lr-pk} + \Delta i_{Lk} = \frac{2C_jV_{\mathrm{in}}}{t_{\mathrm{d}}}, \quad j = 1, 2, 3, 4 \tag{23}$$

From (23), the value of switch output capacitor is obtained as

$$C_j = \frac{(i_{Lr-pk} + \Delta i_{Lk})(t_{\mathrm{d}})}{2V_{\mathrm{in}}}, \quad j = 1, 2, 3, 4 \tag{24}$$

For $i_{Lr-pk} = 0.6875$ A, $\Delta i_{Lk} = 13\%$, $t_d = 100$ ns, and $V_{\mathrm{in}} = 66$ V, the value of C_j is calculated as $C_j = 629$ pF. Hence in order to get the ZVS within 100 ns, the switch output capacitor C_j must be <629 pF.

5 Dimming control and current regulation

Dimming can be achieved by AM or PWM. In AM, dimming is attained by controlling the dc current through LED strings. As LED current is not constant, AM dimming causes chromaticity variations which are undesirable for sensitive lighting applications. Also, AM dimming does not provide a wide dimming range due to non-linear current–voltage characteristics of LED. To avoid

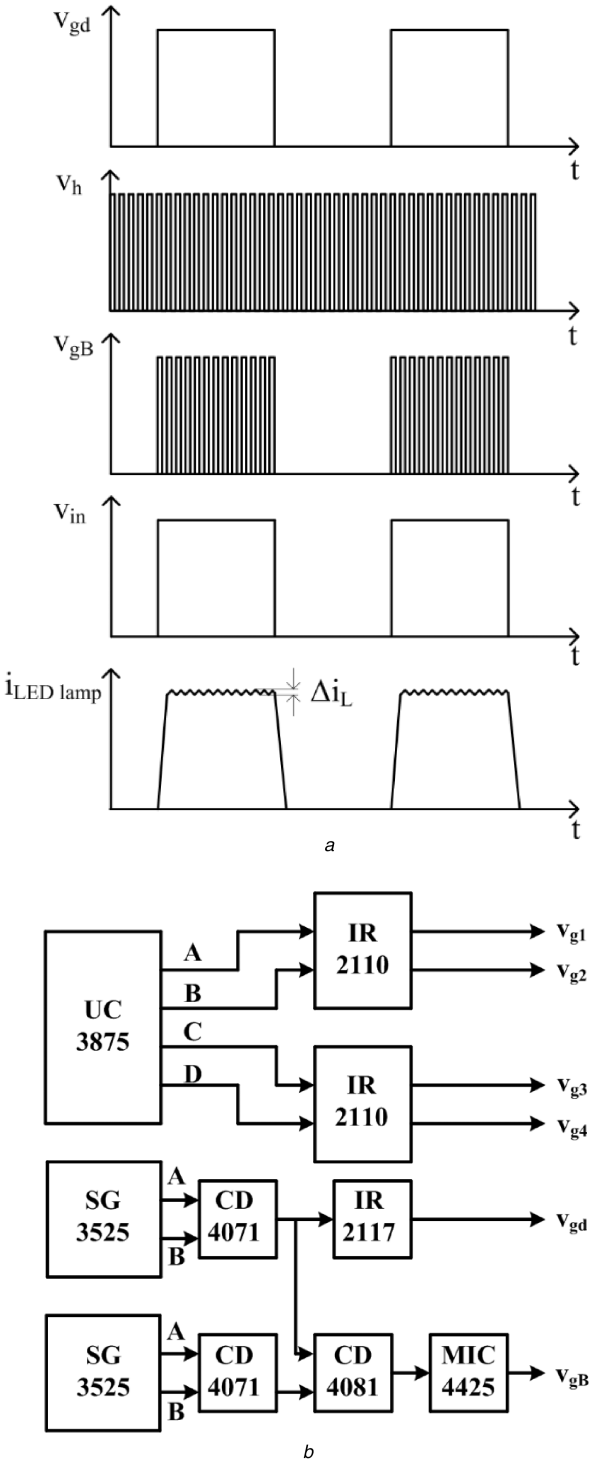

Fig. 4 *Dimming control and control block diagram*

(a) Gate signals of dimming and buck-boost switches, bridge circuit input voltage and LED lamp current,

(b) Block diagram of control circuit of proposed configuration

aforementioned limitations, PWM dimming methods have been widely used. Here, the average current through LED is controlled by turning on and off the LED at a low frequency at nominal current. It offers high dimming range without chromaticity variations and provides smooth dimming. To incorporate dimming into the proposed LED driver, an ON–OFF control switch is connected in series with input dc source. This switch turns ON and OFF the whole converter by using a low-frequency gate signal. Hence, the average current through each LED lamp is changed and brightness of each LED lamp is controlled. The dimming frequency is selected as 100 Hz, to overcome noticeable flickers.

A buck–boost converter is connected in series with input dc source as shown in Fig. 1*a*. In order to regulate LED lamp currents against input voltage variations. This is an essential feature required in battery operated systems. The buck–boost converter is always in operation to provide control over variation in input voltage and its control signal must be synchronised with that of on–off switch. Gate signal (v_{gB}) for switch S_B of buck–boost converter is derived by ANDing a low frequency (100 Hz) control signal (v_{gd}) of dimming switch a high frequency (100 kHz) signal (v_h) as shown in Fig. 4*a*. Bridge input voltage V_{in} and LED lamp current during dimming control are also shown in Fig. 4*a*.

6 Simulation and experimental results

In order to verify the feasibility of the proposed LED driver, a 145 W prototype has been developed. The proposed driver is first simulated using OrCAD PSpice software and then experimental

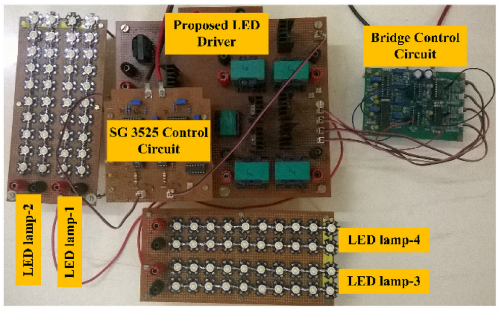

a

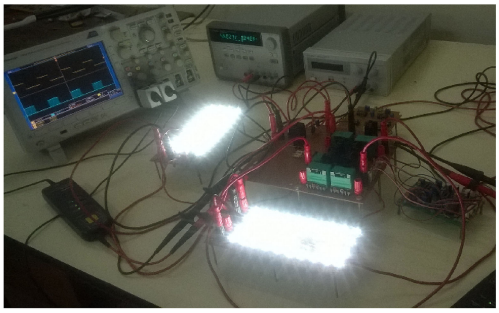

b

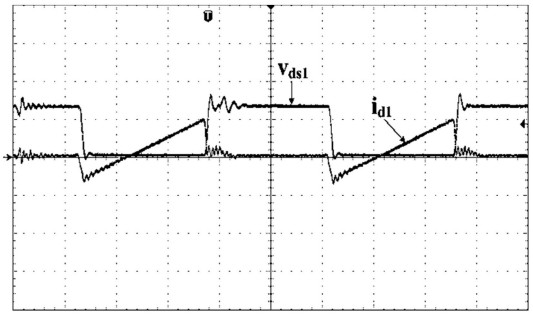

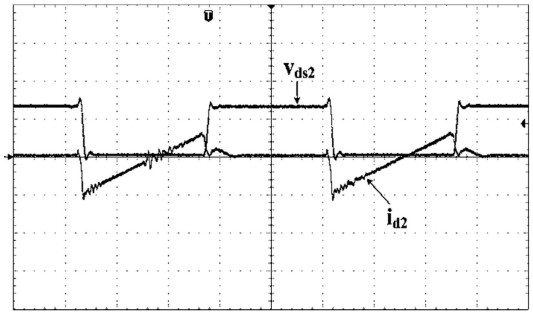

c

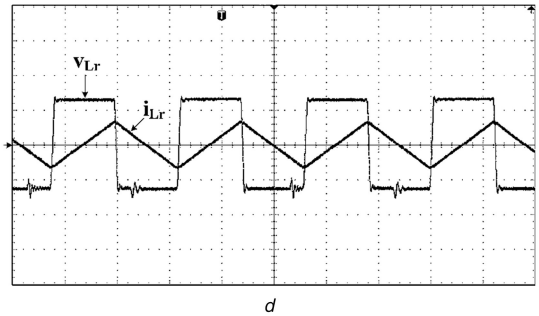

d

Fig. 5 *Experimental prototype of the proposed LED driver and experimental waveforms at full illumination level*

(a) Proposed LED driver with control circuit, ***(b)*** Experimental setup, ***(c)*** Voltage and current in switches S_1 and S_2 (v_{ds1}, v_{ds2}: 50 V/div; i_{d1}, i_{d2}: 1 A/div; time: 1 µs/div), ***(d)*** Voltage and current in L_r (v_{Lr}: 50 V/div; i_{Lr}: 1 A/div; time: 2 µs/div)

prototype has been designed and tested. The parameters of the proposed driver are given in Table 1. For convenience, the dc voltages V_{DC1} and V_{DC2} are selected as 48 and 12 V, respectively. The low input voltage to buck–boost helps in operating it at high duty cycle. The remaining 6 V is supplied by capacitor C. The block diagram of control circuit of proposed circuit is shown in Fig. 4*b*. The picture of the experimental prototype is shown in Figs. 5*a* and *b*. In order to verify the soft switching feature of the driver, experimental switch voltage and switch current waveforms are shown in Fig. 5*c*. The current and voltage across L_r are indicated in Fig. 5*d*. Fig. 6 shows the simulation waveforms of the proposed driver at full illumination level. Fig. 7 shows the corresponding experimental waveforms. It is observed that experimental results are in good agreement with simulation results. It is also observed that switches are turned ON and OFF at zero voltage. With ZVS, switching losses are reduced. Also, switches are conducting only the difference in lamp currents and i_{Lr}. Thus conduction losses are also reduced. Hence the efficiency of the proposed driver is high and efficiency of the driver at full illumination level is found to be 93.88%.

Fig. 8 shows the simulation and experimental results with 60% of dimming control. The switching devices of the bridge configuration are operated at 200 kHz and at a duty cycle of 0.5. The dimming switch and buck–boost switch operations are synchronised to prevent input voltage fluctuations. The input voltage V_{in}, LED lamp currents, and voltages are at their operating values when the dimming switch is ON and they become zero when it is OFF. It is observed that experimental results are in good agreement with simulation results and efficiency is found to be 94.96%.

The proposed LED driver may be applicable to battery operated systems. Consider that dc voltages V_{DC1} and V_{DC2} are obtained through batteries. Fig. 9*a* shows capacitor voltage when $V_{DC1} = 48$ V and $V_{DC2} = 12$ V. Now input voltage to the bridge circuit is 66 V. If the battery voltages are reduced by 5%, i.e. $V_{DC1} = 45.6$ V and $V_{DC2} = 11.4$ V, the capacitor has to compensate the reduction in input voltage, i.e. 9 V. The duty cycle of buck–boost converter is changed accordingly. The corresponding efficiency is found to be 92.46% and capacitor voltage waveform is shown in Fig. 9*b*. Similarly, if the battery voltages are reduced by 10%, the duty cycle is adjusted so that the capacitor can compensate 12 V. Corresponding efficiency is found to be 91.37% and capacitor voltage waveform is shown in Fig. 9*c*. The efficiency curve of the proposed LED driver at various dimming levels is shown in Fig. 9*d*. It is observed that a high efficiency is guaranteed at any dimming level. A relative comparison between H-bridge LED driver topologies and proposed topology is given in Table 2. Proposed configuration does not use high frequency transformer and rectifier stage. It considerably reduces the cost, weight, and volume. Besides, proposed driver circuit features soft switching, reduced current stress and high efficiency with dimming capability.

7 Conclusions

In this paper, a power converter to drive LEDs for high power lighting applications has been developed. It is suitable for street lighting applications. ZVS is obtained in high frequency devices used in a bridge configuration. In addition to this, switches carry a small current which is almost independent of LED lamp currents. Thus switching and conduction losses both are reduced. Dimming can be achieved for all the LED lamps at high efficiency. LED lamp current can be regulated at the desired operating current. High efficiency is guaranteed at any dimming level. This driver eliminates output rectifier stage. It also reduces components count per lamp as well as the cost of the driver. Addition of legs in the bridge to increase the number of lamps is possible in this scheme. The proposed converter may be powered from battery operated systems.

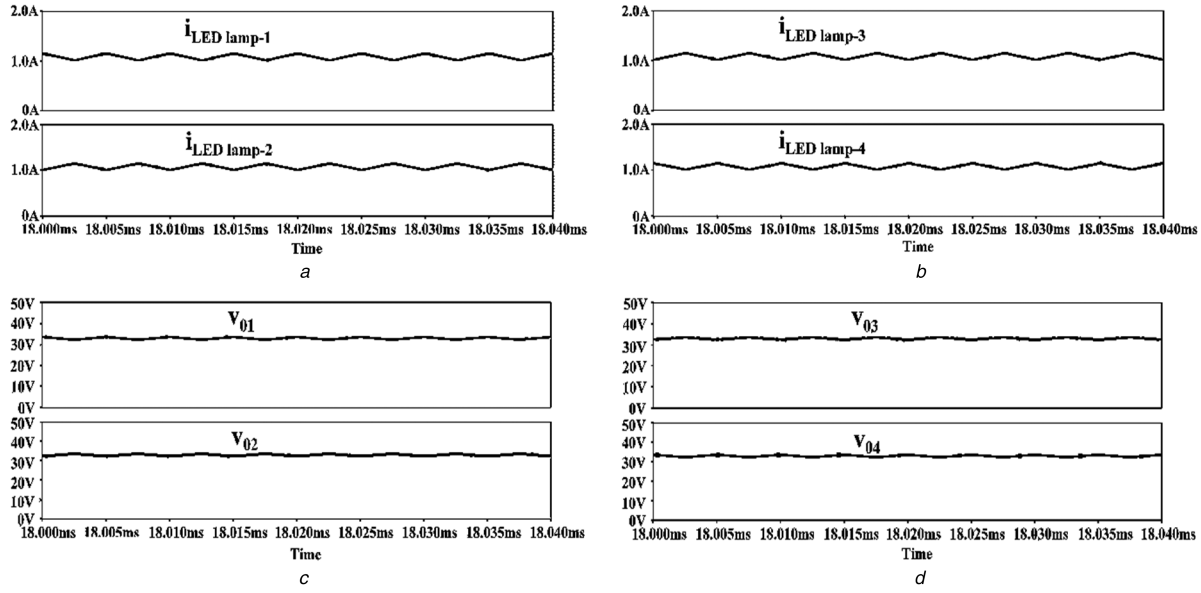

Fig. 6 *Simulation waveforms at full illumination level*
(a) Lamp-1 and Lamp-2 currents, ***(b)*** Lamp-3 and Lamp-4 currents, ***(c)*** Lamp-1 and Lamp-2 voltages, ***(d)*** Lamp-3 and Lamp-4 voltages

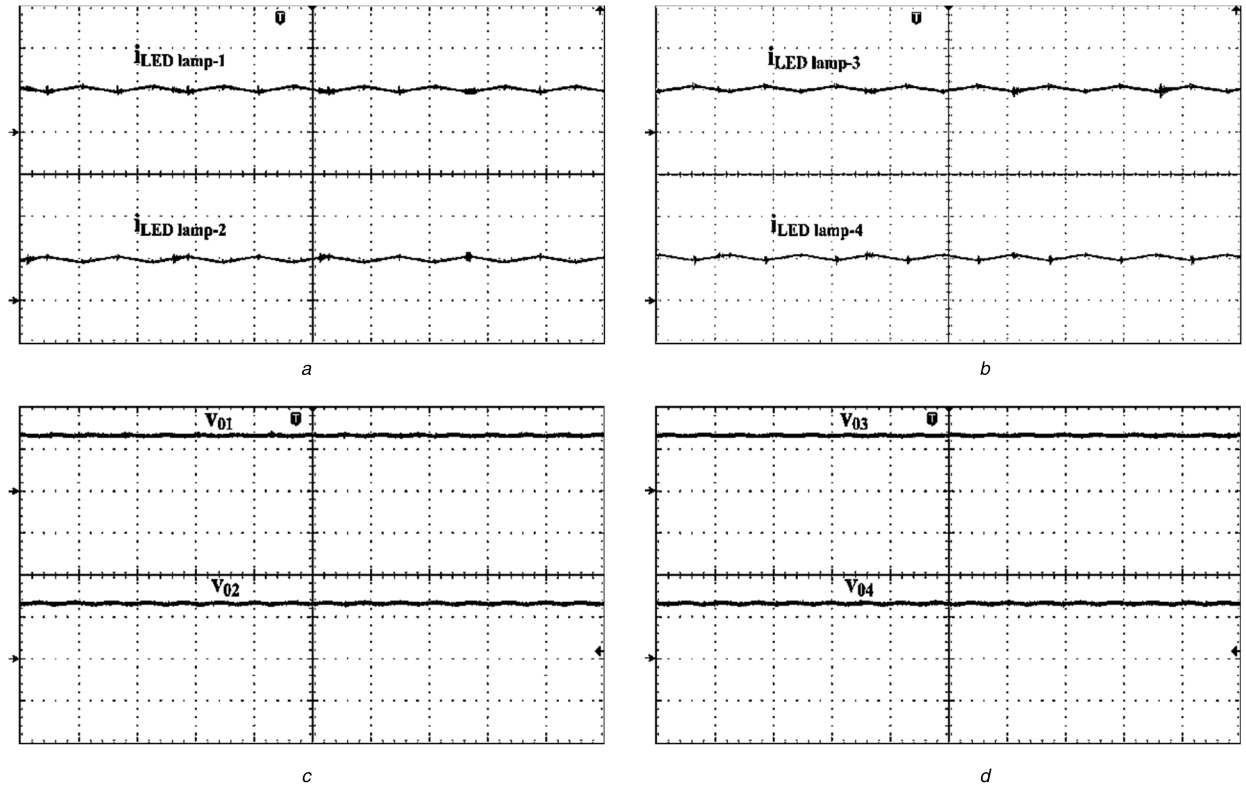

Fig. 7 *Experimental waveforms at full illumination level*
(a) Lamp-1 and Lamp-2 currents (current: 1 A/div; time: 4 μs/div), ***(b)*** Lamp-3 and Lamp-4 currents (current: 1 A/div; time: 4 μs/div), ***(c)*** Lamp-1 and Lamp-2 voltages (voltage: 25 V/div; time: 8 μs/div), ***(d)*** Lamp-3 and Lamp-4 voltages (voltage: 25 V/div; time: 8 μs/div)

Table 1 Parameters of proposed LED driver

DC input voltage, V_{in}	66 V
number of LEDs used	80
LED operating current, $I_{operated}$	550 mA
switching frequency, f_s	200 kHz
duty ratio of switches in bridge configuration	0.5
L_1, L_2, L_3, and L_4	577 μH
L_r	120 μH
PWM dimming frequency	100 Hz
duty ratio of dimming switch S_d	0 to 1
frequency of buck–boost converter	100 kHz
switching devices used	MOSFET IRF640N
control ICs used	UC3875 and SG3525
driver ICs used	IR2110, IR2117, and MIC4425

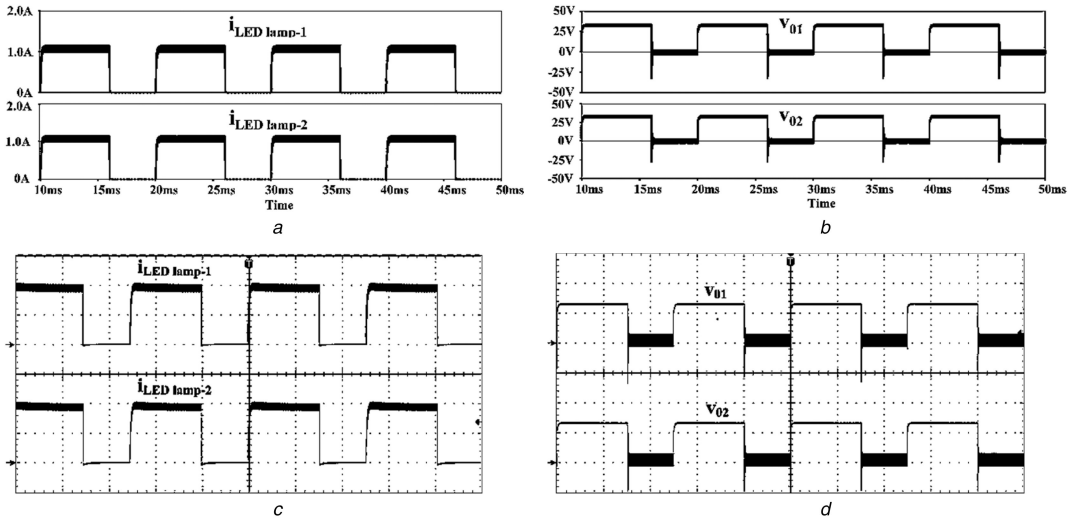

Fig. 8 *Simulation and experimental waveforms with 60% of dimming control*

(a) Simulation waveforms of Lamp-1 and Lamp-2 currents, ***(b)*** Simulation waveforms of Lamp-1 and Lamp-2 voltages, ***(c)*** Experimental waveforms of Lamp-1 and Lamp-2 currents (current: 0.5 A/div; time: 4 ms/div), ***(d)*** Experimental waveforms of Lamp-1 and Lamp-2 voltages (voltage: 25 V/div; time: 4 ms/div)

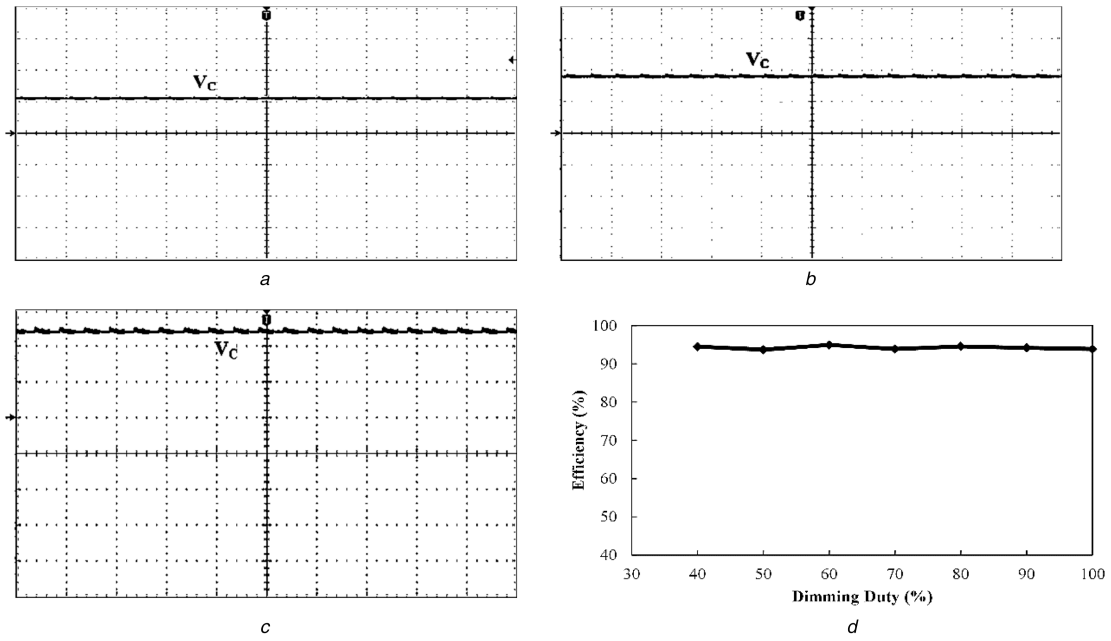

Fig. 9 *Capacitor voltage waveforms and efficiency curve*

(a) V_C under nominal dc voltages (V_C: 5 V/div; time: 20 ms/div), ***(b)*** V_C under 5% discharge (V_C: 5 V/div; time: 20 ms/div), ***(c)*** V_C under 10% discharge (V_C: 5 V/div; time: 20 ms/div), ***(d)*** Efficiency curve under various dimming levels

Table 2 Comparison between H-bridge topologies and proposed topology

H-bridge topology	Brañas *et al.* [23]	Luo *et al.* [24]	Qu *et al.* [25]	Proposed topology
power switches	4	4	6	6
diodes	2	8	4	1
inductors	3	6	2	6
capacitors	3	6	7	1
high frequency transformer	1	1	1	0
high frequency rectifier stage	1	2	4	0
LED lamps	1	2	4	4
efficiency, %	>87	>92	>91	>93

8 References

[1] Ye, Z., Greenfeld, F., Liang, Z.: 'Offline SEPIC converter to drive the high brightness white LED for lighting applications'. Proc. 34th Annual Conf. IEEE Industrial Electronics, Orlando, 2008, pp. 1994–2000

[2] Li, S., Chen, H., Tan, S.C., *et al.*: 'Critical design issues of retrofit light-emitting diode light bulb'. Proc. IEEE Applied Power Electronics Conf. and Exposition APEC-2014, pp. 531–536

[3] Iturriaga-Medina, S., Martinez-Rodriguez, P.R., Juarez-Balderas, , *et al.*: 'A buck converter controller design in an electronic drive for LED lighting applications'. Proc. IEEE Int. Autumn Meeting on Power, Electronics and Computing, Ixtapa, 2015, pp. 1–5

[4] Nuttall, D.R., Shuttleworth, R., Routledge, G.: 'Design of a LED street lighting system'. Proc. 4th IET Conf. Power Electronics, Machines and Drives, York, 2008, pp. 436–440

[5] Crawford, M.H.: 'LEDs for solid-state lighting: performance challenges and recent advances', *IEEE J. Sel. Top. Quantum Electron.*, 2009, **15**, (4), pp. 1028–1040

[6] Cheng, C.A., Chang, C.H., Chung, T.Y., *et al.*: 'Design and implementation of a single-Stage driver for supplying an LED street-Lighting module with power factor corrections', *IEEE Trans. Power Electron.*, 2015, **30**, (2), pp. 956–966

[7] Hui, S.Y., Qin, Y.X.: 'A general photo-electro-thermal theory for light emitting diode (LED) systems', *IEEE Trans. Power Electron.*, 2009, **24**, (8), pp. 1967–1976

[8] Li, S., Tan, S.C., Lee, C.K., *et al.*: 'A survey, classification, and critical review of light-emitting diode drivers', *IEEE Trans. Power Electron.*, 2016, **31**, (2), pp. 1503–1516

[9] Agrawal, A., Jana, K.C., Shrivastava, A.: 'A review of different DC/DC converters for power quality improvement in LED lighting load'. Proc. Int. Conf. Energy Economics and Environment, Noida, 2015, pp. 1–6

[10] Broeck, H.V., Sauerlander, G., Wendt, M.: 'Power driver topologies and control schemes for LEDs'. Proc. 22nd Annual IEEE Applied Power Electronics Conf. and Exposition, Anaheim, 2007, pp. 1319–1325

[11] Hwu, K.I., Tu, W.C., Hong, M.J.: 'A dimmable LED driver based on current balancing transformer with magnetizing energy recycling considered', *J. Disp. Technol.*, 2014, **10**, (5), pp. 388–395

[12] Thomas, W., Pforr, J.: 'Buck-boost converter topology for paralleling HB-LEDs using constant-power operation'. Proc. Int. Conf. Power Electronics and Drive Systems, Taipei, 2009, pp. 568–573

[13] Garcia, J., Calleja, A.J., Corominas, E.L., *et al.*: 'Electronic driver without electrolytic capacitor for dimming high brightness LEDs'. Proc. 35th Annual Conf. IEEE on Industrial Electronics, Porto, 2009, pp. 3518–3523

[14] Fan, S.Y., Tseng, S.Y., Wu, Y.J., *et al.*: 'PV power system using buck/forward hybrid converters for LED lighting'. Proc. IEEE Energy Conversion Congress and Exposition, San Jose, 2009, pp. 2584–2591

[15] Pollock, A., Pollock, H., Pollock, C.: 'High efficiency LED power supply', *IEEE J. Emerg. Sel. Top. Power Electron.*, 2015, **3**, (3), pp. 617–623

[16] Yu, W., Lai, J.S., Ma, H., *et al.*: 'High-efficiency DC–DC converter with twin bus for dimmable LED lighting', *IEEE Trans. Power Electron.*, 2011, **26**, (8), pp. 2095–2100

[17] Garcia, J., Calleja, A.J., Corominas, E.L., *et al.*: 'Interleaved buck converter for fast PWM dimming of high-brightness LEDs', *IEEE Trans. Power Electron.*, 2011, **26**, (9), pp. 2627–2636

[18] Moo, C.S., Chen, Y.J., Yang, W.C.: 'An efficient driver for dimmable LED lighting', *IEEE Trans. Power Electron.*, 2012, **27**, (11), pp. 4613–4618

[19] Jane, G.C., Lin, Y.L., Chiu, H.J., *et al.*: 'Dimmable light-emitting diode driver with cascaded current regulator and voltage source', *IET Power Electron.*, 2015, **8**, (7), pp. 1305–1311

[20] Filho, E.E.S., Miranda, P.H.A., Sá, E.M., *et al.*: 'A LED driver with switched capacitor', *IEEE Trans. Ind. Appl.*, 2014, **50**, (5), pp. 3046–3054

[21] Wang, Y., Guan, Y., Xu, D., *et al.*: 'A CLCL resonant DC/DC converter for Two-Stage LED driver system', *IEEE Trans. Ind. Electron.*, 2016, **63**, (5), pp. 2883–2891

[22] Chansri, P., Noicharoen, N., Phetphoi, K.: 'A high power LED driver with Class-D ZVS series resonant converter'. Int. Conf. Electrical, Control and Computer Engineering, Pahang, 2011, pp. 457–460

[23] Brañas, C., Azcondo, F.J., Casanueva, R., *et al.*: 'Phase-controlled parallel-series (LCpCs) resonant converter to drive high-brightness power LEDs'. 37th Annual Conf. IEEE Industrial Electronics Society, Melbourne, 2011, pp. 2953–2957

[24] Luo, Q., Zhi, S., Zou, C., *et al.*: 'Analysis and design of a multi-channel constant current light-emitting diode driver based on high-frequency AC bus', *IET Power Electron.*, 2013, **6**, (9), pp. 1803–1811

[25] Qu, X., Wong, S.C., Tse, C.K.: 'An improved LCLC current-source-output multistring LED driver with capacitive current balancing', *IEEE Trans. Power Electron.*, 2015, **30**, (10), pp. 5783–5791

[26] Qu, X., Wong, S.C., Tse, C.K.: 'Resonance-Assisted buck converter for offline driving of power LED replacement lamps', *IEEE Trans. Power Electron.*, 2011, **26**, (2), pp. 532–540

[27] Ye, A., Greenfeld, F., Liang, Z.: 'Single-stage offline SEPIC converter with power factor correction to drive high brightness LEDs'. Proc. IEEE Applied Power Electronics Conf. and Exposition, 2009, pp. 546–553

[28] Loo, K.H., Lun, W.K., Tan, S.C., *et al.*: 'On driving techniques for LEDs: toward a generalized methodology', *IEEE Trans. Power Electron.*, 2009, **24**, (12), pp. 2967–2976

[29] Chiu, H.J., Lo, Y.K., Chen, J.T., *et al.*: 'A high-Efficiency dimmable LED driver for Low-Power lighting applications', *IEEE Trans. Ind. Electron.*, 2010, **57**, (2), pp. 735–743

[30] Bęczkowski, S., Munk-Nielsen, S.: 'LED spectral and power characteristics under hybrid PWM/AM dimming strategy'. Proc. IEEE Energy Conversion Congress and Exposition, Atlanta, 2010, pp. 731–735

[31] Doshi, M., Zane, R.: 'Control of solid-State lamps using a multiphase pulsewidth modulation technique', *IEEE Trans. Power Electron.*, 2010, **25**, (7), pp. 1894–1904

[32] Chang, Y.H., Chen, Y.J., Chuang, Y.C., *et al.*: 'Driving circuit for high-brightness LED lamps'. Proc. Int. Power Electronics Conf., Sapporo, 2010, pp. 403–407

[33] Lun, W.K., Loo, K.H., Tan, S.C., *et al.*: 'Bilevel current driving technique for LEDs', *IEEE Trans. Power Electron.*, 2009, **24**, (12), pp. 2920–2932

[34] Vishwanathan, N., Porpandiselvi, S., Ramakrishnareddy, K.: Indian Patent Application, 201641038698, 2016

[35] Rodrigues, W.A., Morais, L.M.F., Donoso-Garcia, P.F., *et al.*: 'Comparative analysis of power LEDs dimming methods'. XI Brazilian Power Electronics Conf., Praiamar, 2011, pp. 378–383

[36] Henze, C.P., Martin, H.C., Parsley, D.W.: 'Zero-voltage switching in high frequency power converters using pulse width modulation'. Proc. Third Annual IEEE APE Conf. and Exposition, New Orleans, 1988, pp. 33–40